

# Non-equilibrium current and relaxation dynamics of a charge-fluctuating quantum dot

C. KARRASCH<sup>1(a)</sup>, S. ANDERGASSEN<sup>1</sup>, M. PLETYUKHOV<sup>1</sup>, D. SCHURICHT<sup>1</sup>, L. BORDA<sup>2</sup>, V. MEDEN<sup>1</sup>  
and H. SCHOELLER<sup>1</sup>

<sup>1</sup> *Institut für Theoretische Physik A and JARA-Fundamentals of Future Information Technology, RWTH Aachen University - D-52056 Aachen, Germany, EU*

<sup>2</sup> *Physikalisches Institut, Universität Bonn - D-53115 Bonn, Germany, EU*

received 11 March 2010; accepted in final form 22 April 2010  
published online 27 May 2010

PACS 05.60.Gg – Quantum transport

PACS 71.10.-w – Theories and models of many-electron systems

PACS 73.63.Kv – Electronic transport in nanoscale materials and structures: Quantum dots

**Abstract** – We study the steady-state current in a minimal model for a quantum dot dominated by charge fluctuations and analytically describe the time evolution into this state. The current is driven by a finite-bias voltage  $V$  across the dot, and two different renormalization group methods are used to treat small-to-intermediate local Coulomb interactions. The corresponding flow equations can be solved analytically, which allows to identify all microscopic cutoff scales. Exploring the entire parameter space we find rich non-equilibrium physics which cannot be understood by simply considering the bias voltage as an infrared cutoff. For the experimentally relevant case of left-right asymmetric couplings, the current generically shows a power law suppression for large  $V$ . The relaxation dynamics towards the steady state features characteristic oscillations as well as an interplay of exponential and power law decay.

Copyright © EPLA, 2010

**Introduction.** – Recent progress in the ability to engineer nanostructured devices has opened new possibilities for studying the finite-bias transport characteristics of such systems. As the electrons occupying the nanostructure are spatially confined, local Coulomb correlations strongly affect the physics, and understanding non-equilibrium phenomena in systems with local two-particle interactions is therefore of fundamental importance. In an attempt to investigate simplified cases first, one can distinguish between situations in which either charge or spin fluctuations dominate. The latter case is described by the Kondo model, and progress in understanding its non-equilibrium physics was made recently (for a review see ref. [1]). We here consider the other situation and study a minimal model for a quantum dot dominated by charge fluctuations —the interacting resonant level model (IRLM). It describes a spinless localized level at energy  $\epsilon$  coupled to two leads by electron hoppings  $t_\alpha$  and local Coulomb repulsions  $u_\alpha$  (see fig. 1). The lead electrons are assumed to be (effectively) non-interacting and held

at two different chemical potentials  $\mu_\alpha = \pm V/2$ , with  $\alpha = L, R$  denoting the left and right lead and  $V$  being the bias voltage.

The steady-state current  $I$  of the IRLM was studied intensively during the last few years using various techniques including the scattering Bethe Ansatz [2], perturbative and numerical renormalization group (NRG) methods [3], the Hershfield  $Y$ -operator [4], the time-dependent density matrix renormalization group (tDMRG) method [5] as well as sophisticated field theory approaches [5,6]. These studies were mostly performed at the non-generic point of particle-hole and left-right symmetry, which can hardly be realized in experiments. It was concluded that at sufficiently large  $V$ ,  $I$  decreases as a power law. Similar power laws were found in equilibrium and it was suggested that  $V$  is just another infrared energy cutoff (in addition to, *e.g.*,  $t_\alpha$  or temperature), leading to the speculation that the IRLM does not contain any interesting non-equilibrium physics [3]. Exploring the entire parameter space we show analytically that this conclusion is too restrictive. We uncover rich non-equilibrium physics beyond the situation where the

<sup>(a)</sup>E-mail: karrasch@physik.rwth-aachen.de

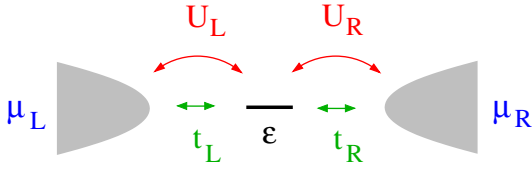


Fig. 1: (Color online) The interacting resonant level model discussed in this work.

voltage  $V$  acts as a simple low-energy cutoff associated with a power law behavior of the current. However, in the limit of strong left-right asymmetry, which can be easily realized experimentally, we find generic power law scaling of  $I$  for large  $V$ , in particular also away from particle-hole symmetry.

In addition, we provide an analytic description of the relaxation dynamics of the system into the steady state after switching on the level-lead coupling at time  $t = 0$ . Two different relaxation rates control the exponential decay which is accompanied by oscillatory behavior with a voltage-dependent frequency and power law decay with an exponent depending on  $u_\alpha$ . Describing the time evolution of a locally correlated electron system is as challenging as understanding the non-equilibrium steady-state current. Various numerical techniques like time-dependent NRG [7] and tDMRG [8], an iterative path-integral method [9], and a non-equilibrium Monte Carlo approach [10] were developed. Certain exactly solvable models were discussed [11], and a perturbative renormalization group (RG) method [12,13] as well as a flow equation approach [14] were applied. However, these studies do not cover charge-fluctuating, correlated quantum dots.

In this letter, we use two RG methods to investigate the IRLM. While both are bound to the case of weak Coulomb interactions, they are complementary in other aspects. Within the functional RG (FRG), which was recently extended to non-equilibrium [15], the steady state can be studied for arbitrary system parameters. In particular, this allows for a comparison to highly accurate tDMRG data obtained for hoppings which are too large to be deep in the scaling limit [5], the latter being realized for large band width and small  $t_\alpha$ . For small interactions, we find excellent agreement (see fig. 3(a)). In the scaling limit, the FRG results and the ones obtained by the real-time renormalization group in frequency space (RTRG-FS) [1] coincide (see figs. 2 and 4). The latter method was earlier applied to systems dominated by spin fluctuations [16]. In contrast to the FRG, RTRG-FS can only be used in the scaling limit, but, on the other hand, it allows for an analytical description not only of the steady state but also of the relaxation dynamics. The combined use of both RG approaches leads to a reliable and comprehensive picture of the non-equilibrium physics under consideration. In particular, we identify the various microscopic cutoff scales, which is essential for the precise determination of the scaling behavior of observables.

**Model and RG equations.** – The Hamiltonian of the IRLM (see fig. 1) is given by  $H = H_l + H_d + H_c$ , where  $H_l = \sum_{k\alpha} (\epsilon_k + \mu_\alpha) a_{k\alpha}^\dagger a_{k\alpha}$  describes two semi-infinite fermionic leads which are held at  $\mu_{L/R} = \pm V/2$ , respectively. A standard second quantized notation is used, and the energies  $\epsilon_{k\alpha}$  are restricted to a finite band of width  $B$ . In the scaling limit, the details of the frequency dependence of the lead local density of states  $\rho_\alpha$  do not play any role as long as it is sufficiently regular for energies of the order of  $V$  and smaller. When comparing to tDMRG data [5], we employ the semi-circular  $\rho_\alpha(\omega)$  associated with simple tight-binding chains (which are used in tDMRG). The dot Hamiltonian reads  $H_d = \epsilon \hat{n}$  with  $\hat{n} = c^\dagger c$ , and this single fermionic level is coupled to the leads via  $H_c = \sum_{k\alpha} t_\alpha (a_{k\alpha}^\dagger c + \text{H.c.}) + (\hat{n} - \frac{1}{2}) \sum_{kk'\alpha} u_\alpha \cdot a_{k\alpha}^\dagger a_{k'\alpha}$ , where  $\cdot \dots \cdot$  denotes normal-ordering. We stress that in contrast to other studies, the coupling to the leads is allowed to be asymmetric, which is the situation generically expected in experiments. Furthermore, we do not only focus on the particle-hole symmetric point  $\epsilon = 0$ .

Within both RG approaches, coupled differential equations for the flow of the effective system parameters as a function of an infrared cutoff  $\Lambda$  holding up to leading order in  $u_\alpha$  can be derived. Aiming at an analytic discussion, it is instructive to consider *simplified* flow equations for the renormalized steady-state rates  $\Gamma_\alpha$  whose bare values are given by  $\Gamma_\alpha^0 = 2\pi\rho_\alpha t_\alpha^2$ . In the scaling limit, both RG approaches give the same functional form

$$\frac{d\Gamma_\alpha}{d\Lambda} = -2U_\alpha \Gamma_\alpha \frac{\Lambda + \Gamma/2}{(\mu_\alpha - \epsilon)^2 + (\Lambda + \Gamma/2)^2}, \quad (1)$$

with  $U_\alpha = \rho_\alpha u_\alpha$  being the dimensionless interaction, and  $\Gamma = \sum_\alpha \Gamma_\alpha$ . The renormalization of the level position  $\epsilon$  is small and will be neglected. The RG flow 1 is cut off at the scale  $\Lambda_c = \max\{|\mu_\alpha - \epsilon|, \Gamma/2\}$ , and an approximate solution for  $\Gamma_\alpha$  is given by

$$\Gamma_\alpha = \Gamma_\alpha^0 \left( \frac{\Lambda_0}{\Lambda_c} \right)^{2U_\alpha}, \quad (2)$$

where  $\Lambda_0 \sim B$  denotes the initial cutoff. At large voltages  $V \gg \Gamma$ , we distinguish between the *off-resonance*  $|V - 2\epsilon| > \Gamma$  and the *on-resonance*  $V = 2\epsilon$  situation (peak in conductance; see fig. 4). In the latter case, the relevant energy scales cutting off the flow are  $\Gamma/2$  for  $\Gamma_L$  and  $V$  for  $\Gamma_R$ .

Similar to the Kondo model the cutoff parameter is the maximum of the distance to the resonance and the corresponding decay rate, *i.e.* in our case  $\max\{|\epsilon \pm V/2|, \Gamma\}$ . There is, however, an important difference. For the Kondo model, even at resonance  $V = \hbar$  (the latter being the magnetic field), there is a weak-coupling expansion parameter, namely the dimensionless exchange coupling cut off at  $\max(V, \hbar)$ . For the IRLM, at  $\epsilon = \pm V/2$ , the tunneling is not a weak-coupling expansion parameter since  $\Gamma$  is not dimensionless. This fact constitutes an essential

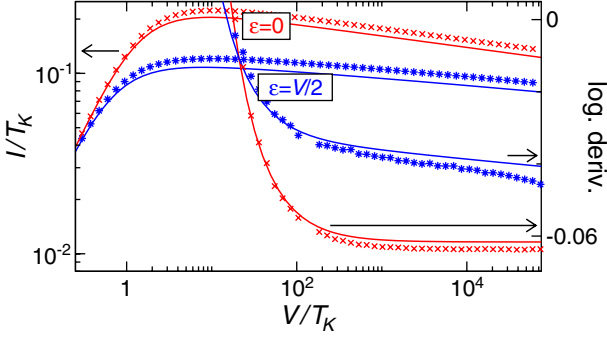


Fig. 2: (Color online)  $I(V)$  for the symmetric model with  $U_L = U_R = 0.1/\pi$  obtained from the numerical solution of the full RTRG-FS (lines) and FRG (symbols) equations; crosses:  $\epsilon = 0$ ; stars:  $\epsilon = V/2$ .

difference between the description of resonance phenomena in models with charge and spin fluctuations.

The *full* FRG and RTRG-FS flow equations are presented in refs. [17] and [18], respectively, and can easily be solved on a computer. If not mentioned otherwise, the results shown in the figures were obtained in this way (for a comparison to the analytic solution of the simplified equations see fig. 3(b)).

In the scaling limit where  $\Lambda_0 \rightarrow \infty$  and  $\Gamma_\alpha^0 \rightarrow 0$ , the dependence on bare parameters vanishes, and all quantities can be expressed in terms of the invariant scale  $T_K = \sum_\alpha T_K^\alpha$ , with  $T_K^\alpha = \Gamma_\alpha^0 (2\Lambda_0/T_K)^{2U_\alpha}$ , and the asymmetry parameter  $c^2 = T_K^L/T_K^R$ . Thus, at  $V = 0$

$$\Gamma = T_K \left[ c \left( \frac{T_K}{\Gamma} \right)^{2U_L} + \frac{1}{c} \left( \frac{T_K}{\Gamma} \right)^{2U_R} \right] \frac{c}{1+c^2}, \quad (3)$$

which has the solution  $\Gamma = T_K$  in the symmetric case ( $U_L = U_R$ ,  $c = 1$ ). The corresponding equation for  $\Gamma$  at finite  $V$  in the off- (on-) resonance situation is obtained by replacing  $\Gamma$ 's on the right-hand side of (3) by  $V - 2\epsilon$  and  $V + 2\epsilon$  (by  $\Gamma$  and  $2V$ ). As a result, the rates  $\Gamma_\alpha$  are generically characterized by power laws with interaction-dependent exponents.

**Steady-state quantities.** – The dot occupation in the stationary state reads

$$\langle \hat{n} \rangle = \frac{1}{2} + \frac{1}{\pi} \left[ \frac{\Gamma_L}{\Gamma} \arctan \frac{V-2\epsilon}{\Gamma} - \frac{\Gamma_R}{\Gamma} \arctan \frac{V+2\epsilon}{\Gamma} \right], \quad (4)$$

and the static susceptibility is defined as  $\chi = -\frac{\partial \langle \hat{n} \rangle}{\partial \epsilon} |_{\epsilon=0}$ .

In the symmetric case and at  $V = 0$ , one obtains  $\chi_{V=0}^{\text{sym}} = 2/(\pi\Gamma)$  (see footnote <sup>1</sup>) which can be used to define the physical scale  $T_K = \frac{2}{\pi} (\chi_{V=0}^{\text{sym}})^{-1}$  even away from the scaling limit. The stationary current can directly be computed

<sup>1</sup>The power law scaling of  $\chi_{V=0}^{\text{sym}}$  as a function of  $\Gamma_L^0 = \Gamma_R^0$  [3] is captured both by FRG and RTRG-FS in good agreement with NRG data.

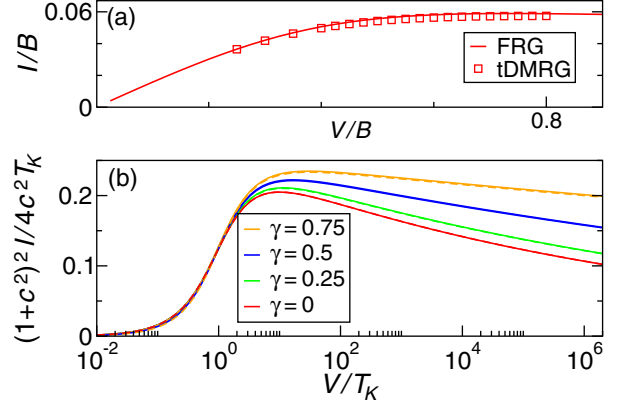


Fig. 3: (Color online) (a) Comparison of FRG results (lines) and tDMRG data [5] (symbols) of  $I(V)$  for  $u_L = u_R = 0.3B/4$  and  $t_L = t_R = 0.5B/4$  at  $\epsilon = 0$ . (b) RTRG-FS results for  $I(V)$  for  $U_{L/R} = (1 \pm \gamma) 0.1/\pi$ , and  $\epsilon = 0$ ; the analytic result (2) inserted in (5) (dashed lines) is mostly hidden by the solution of the full flow equations (solid lines);  $\gamma = 0.75, 0.5, 0.25, 0$  (corresponding to  $c^2 = 21.4, 7.9, 2.8, 1$ ) from top to bottom.

from the rates  $\Gamma_\alpha$ :

$$I = \frac{1}{\pi} \frac{\Gamma_L \Gamma_R}{\Gamma} \left[ \arctan \frac{V-2\epsilon}{\Gamma} + \arctan \frac{V+2\epsilon}{\Gamma} \right]. \quad (5)$$

For  $V \gg \Gamma$  and *off resonance*, this expression simplifies to  $I \approx \Gamma_L \Gamma_R / \Gamma$  and thus

$$I(V) \approx T_K \frac{\left( \frac{T_K}{|V-2\epsilon|} \right)^{2U_L} \left( \frac{T_K}{|V+2\epsilon|} \right)^{2U_R}}{c \left( \frac{T_K}{|V-2\epsilon|} \right)^{2U_L} + \frac{1}{c} \left( \frac{T_K}{|V+2\epsilon|} \right)^{2U_R}} \frac{c}{1+c^2}. \quad (6)$$

Whereas for  $U_L = U_R = U$  and  $V \gg \epsilon$  (*e.g.*, at the particle-hole symmetric point  $\epsilon = 0$ ) the current is always governed by a power law  $I(V) \propto V^{-2U}$  in agreement with earlier studies [4,5], this does not hold in general for asymmetric Coulomb interactions generically realized in experiments. In this case the two terms in the denominator of (6) are typically of the same order of magnitude. Only if in addition to  $U_L \neq U_R$  the asymmetry in the bare rates is large ( $c \ll 1$  or  $c \gg 1$ ), the power law behavior of  $I(V)$  is recovered (with exponents  $2U_L$  or  $2U_R$ , respectively). In the *on-resonance* case  $\epsilon = V/2$  where the conductance  $G = dI/dV$  has a maximum (see fig. 4), the current is given by

$$I(V) \approx \frac{\Gamma_L \Gamma_R}{2\Gamma} = \frac{T_K}{2} \frac{\left( \frac{T_K}{\Gamma} \right)^{2U_L} \left( \frac{T_K}{2V} \right)^{2U_R}}{c \left( \frac{T_K}{\Gamma} \right)^{2U_L} + \frac{1}{c} \left( \frac{T_K}{2V} \right)^{2U_R}} \frac{c}{1+c^2}. \quad (7)$$

In contrast to the off-resonance situation,  $I$  does not follow a power law even in the left-right symmetric model (see fig. 2). Only for very large  $V$  (or for  $c \gg 1$ ), the second term in the denominator of (7) can be neglected and  $I \propto V^{-2U_R}$  (see footnote <sup>2</sup>). Thus, the voltage  $V$

<sup>2</sup>In contrast, the perturbative study of ref. [4] yields  $I \propto V^{-U}$ , with  $U = U_L = U_R$ .

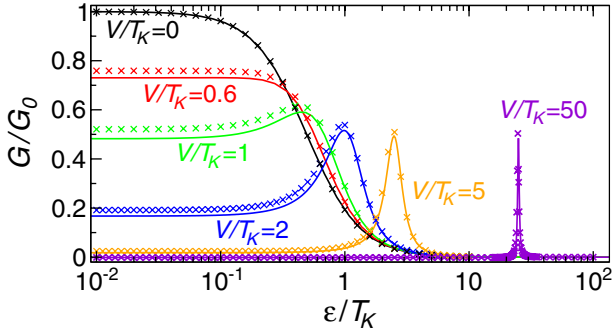


Fig. 4: (Color online) Conductance  $G(\epsilon) = dI/dV$  (lines: RTRG-FS; symbols: FRG) in the symmetric model with  $U_L = U_R = 0.1/\pi$ .

cannot be interpreted as a simple infrared cutoff both for  $\epsilon = \pm V/2$  and  $U_L \neq U_R$  and the physics in non-equilibrium is far more complex than in the linear-response limit<sup>3</sup>.

The analytic results (2), (6), and (7) derived from approximate FRG and RTRG-FS flow equations are confirmed by solving the full RG equations numerically. The current for the left-right symmetric model exhibits a power law decay  $I \propto V^{-2U}$  and thus a constant logarithmic derivative only in the off-resonance case (see fig. 2). Figure 3(b) illustrates for  $\epsilon = 0$  and different coupling asymmetries that the current from the full RTRG-FS flow equation is captured by the analytic solution for the rates (2) inserted in (5). Moreover, the FRG compares nicely with accurate tDMRG reference results obtained for large hoppings (see fig. 3(a)). Another transport property of experimental interest is the conductance  $G$ , which as a function of the gate voltage  $\epsilon$  most importantly features the mentioned resonance at  $\epsilon = \pm V/2$  as the voltage becomes large (see fig. 4). As before, both RG frameworks give agreeing numerical results for arbitrary values of  $V/T_K$  and  $\epsilon/T_K$ , thus altogether providing reliable tools to study quantum dot systems out of equilibrium.

**Time evolution.** – The RTRG-FS allows for studying the time evolution towards the steady state. To this end, we initially prepare the system in a state described by  $\hat{\rho}(t < 0) = \hat{\rho}_D^{(0)} \hat{\rho}_L \hat{\rho}_R$ , where  $\hat{\rho}_D^{(0)}$  is an arbitrary initial density matrix of the dot and  $\hat{\rho}_{L/R}$  are grandcanonical distributions of the leads. At time  $t = 0$ , the coupling  $H_c$  is suddenly switched on and transient dynamics of  $\hat{\rho}_D$  sets in. The latter can be fully described in terms of  $\Gamma_\alpha$  as a function of a Laplace variable  $z$  which has to be incorporated [18]. By analytically solving an approximation to these RG equations, one can obtain closed integral representations both for the dot occupation  $\langle \hat{n}(t) \rangle$  and the

<sup>3</sup>In quantum dot transport experiments, the bandwidth  $B \sim 1$  eV is typically large compared to the Kondo scale  $T_K \sim 0.2$  meV which is in turn larger than the usual environment temperature  $T \sim 0.02$  meV. Thus, the regime of negative differential conductance of the IRLM is roughly associated with a current of the order of  $I \sim 0.5$  nA and voltages  $V \sim 20$  meV.

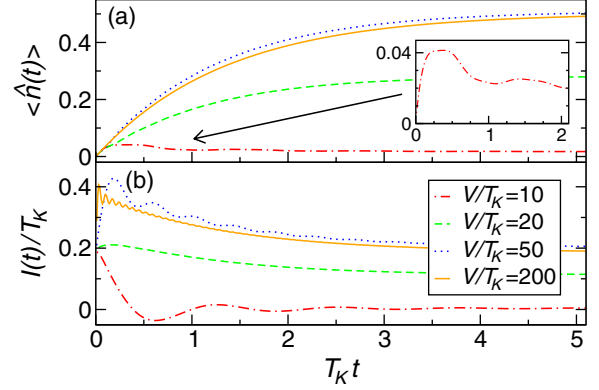


Fig. 5: (Color online) Time evolution of the dot occupation  $\langle \hat{n}(t) \rangle$  and the current  $I(t)$  for  $U_L = U_R = 0.1/\pi$ ,  $\epsilon = 10 T_K$ , and the initial condition  $\langle \hat{n}(0) \rangle = 0$  (see footnote <sup>4</sup>). At times  $t \lesssim 2/T_K$  we observe an oscillating behavior.

current  $I(t)$  by virtue of inverse Laplace transform [13]. Numerical results for the time evolution are shown in fig. 5. We restrict ourselves to the left-right symmetric model for simplicity. The long-time behavior away from resonance (*i.e.*, at  $\epsilon, V, |\epsilon - V/2| \gg T_K, 1/t$ ) is given by

$$\begin{aligned} \langle \hat{n}(t) \rangle &\approx (1 - e^{-\Gamma_1 t}) \langle \hat{n} \rangle - \frac{1}{2\pi} e^{-\Gamma_2 t} (T_K t)^{1+2U} \\ &\times \left[ \frac{\sin[(\epsilon + \frac{V}{2})t]}{(\epsilon + \frac{V}{2})^2 t^2} - \frac{\pi U \cos[(\epsilon + \frac{V}{2})t]}{4 (\epsilon + \frac{V}{2})^2 t^2} + (V \rightarrow -V) \right], \end{aligned} \quad (8)$$

where  $\langle \hat{n} \rangle$  follows from (4), and  $\Gamma_1 \approx \Gamma$  as well as  $\Gamma_2 \approx \Gamma_1/2$  are two decay rates. Whereas  $\Gamma_1$  describes the charge relaxation process,  $\Gamma_2$  is the broadening of the local level  $\epsilon$  induced by the coupling to the leads, *i.e.* it describes the relaxation of nondiagonal elements of the local density matrix with respect to the charge states. We note that the dephasing rate  $\Gamma_\phi = \Gamma_2 - \Gamma_1/2 \sim \mathcal{O}(U)$  is due to pure potential fluctuations on the dot and increases for large Coulomb interactions. Most notable characteristics of the time evolution of both  $\langle \hat{n}(t) \rangle$  as well as the current  $I(t)$  are that i) the relaxation towards the stationary value is governed by both decay rates, ii) the voltage appears as an important energy scale for the dynamics setting the frequency of an oscillatory behavior, and iii) the exponential decay is accompanied by an algebraic decay  $\propto t^{2U-1}$ . The last result is of particular importance for applications in error correction schemes of quantum information processing as it contrasts the standard assumption of a purely exponential decay [19]. We also note that in the short-time dynamics a reversal of the current can occur (see the dash-dotted curve in fig. 5(b)). This effect is due to very strong charge fluctuations in the transient state, thus being impossible

<sup>4</sup>The current in the lead at times  $t \sim 1/B$  is determined by the nonzero displacement current  $d\langle \hat{n}(t) \rangle/dt$ .

in systems with spin or orbital fluctuations [13]. Another interesting observation is that in the resonance case (dashed line) current oscillations are fully damped.

**Conclusion.** – We have studied non-equilibrium transport properties of a spinless single-level quantum dot coupled to leads via tunneling and Coulomb interaction, representing a fundamental model to describe the effects of charge fluctuations. Using two different RG methods we have presented analytic results in the entire parameter regime and concluded that the steady-state current  $I(V)$  exhibits a power law only in specific cases. The one of highest experimental relevance is the situation of strong asymmetries in the tunneling couplings, where we generically observed a power law for large bias voltages  $V$ . Furthermore, the time evolution towards the steady state was studied. We found exponential decay on two different scales accompanied by voltage-dependent oscillations and power laws with interaction-dependent exponents.

\*\*\*

We thank P. SCHMITTECKERT for providing the DMRG data of ref. [5], and N. ANDREI, B. DOYON, A. TSVELIK, and A. ZAWADOWSKI for discussions. This work was supported by the DFG-FG 723 and 912, and by the AHV.

#### REFERENCES

- [1] SCHOELLER H., *Eur. Phys. J. ST*, **168** (2009) 179.
- [2] MEHTA P. and ANDREI N., *Phys. Rev. Lett.*, **96** (2006) 216802; arXiv:cond-mat/0703246 (Erratum).
- [3] BORDA L., VLADÁR K. and ZAWADOWSKI A., *Phys. Rev. B*, **75** (2007) 125107.
- [4] DOYON B., *Phys. Rev. Lett.*, **99** (2007) 076806.
- [5] BOULAT E., SALEUR H. and SCHMITTECKERT P., *Phys. Rev. Lett.*, **101** (2008) 140601.
- [6] BOULAT E. and SALEUR H., *Phys. Rev. B*, **77** (033409) 2008.
- [7] ANDERS F. and SCHILLER A., *Phys. Rev. Lett.*, **95** (196801) 2005.
- [8] DALEY A. *et al.*, *J. Stat. Mech.* (2004) P04005; WHITE S. and FEIGUIN A., *Phys. Rev. Lett.*, **93** (2004) 076401; SCHMITTECKERT P., *Phys. Rev. B*, **70** (2004) 121302; HEIDRICH-MEISNER F., FEIGUIN A. and DAGOTTO E., *Phys. Rev. B*, **79** (2009) 235336.
- [9] WEISS S. *et al.*, *Phys. Rev. B*, **77** (2008) 195316.
- [10] SCHMIDT T. *et al.*, *Phys. Rev. B*, **78** (2008) 235110.
- [11] LESAGE F. and SALEUR H., *Phys. Rev. Lett.*, **80** (1998) 4370; SCHILLER A. and HERSHFELD S., *Phys. Rev. B*, **62** (2000) R16271; KOMNIK A., *Phys. Rev. B*, **79** (2009) 245102.
- [12] KEIL M. and SCHOELLER H., *Phys. Rev. B*, **63** (2001) 180302(R).
- [13] PLETYUKHOV M., SCHURICHT D. and SCHOELLER H., *Phys. Rev. Lett.*, **104** (2010) 106801.
- [14] LOBASKIN D. and KEHREIN S., *Phys. Rev. B*, **71** (2005) 193303; HACKL A. *et al.*, *Phys. Rev. Lett.*, **102** (2009) 196601; HACKL A., VOJTA M. and KEHREIN S., *Phys. Rev. B*, **80** (2009) 195117.
- [15] GEZZI R., PRUSCHKE TH. and MEDEN V., *Phys. Rev. B*, **75** (2007) 045324; JAKOBS S., MEDEN V. and SCHOELLER H., *Phys. Rev. Lett.*, **99** (2007) 150603; SCHMIDT H. and WÖLFLE P., *Ann. Phys. (Berlin)*, **19** (2010) 60; JAKOBS S., PLETYUKHOV M. and SCHOELLER H., *Phys. Rev. B*, **81** (2010) 195109.
- [16] SCHOELLER H. and REININGHAUS F., *Phys. Rev. B*, **80** (2009) 045117; SCHURICHT D. and SCHOELLER H., *Phys. Rev. B*, **80** (2009) 075120.
- [17] KARRASCH C., PLETYUKHOV M., BORDA L. and MEDEN V., *Phys. Rev. B*, **81** (2010) 125122.
- [18] ANDERGASSEN S. *et al.*, in preparation.
- [19] PESKILL J., in *Introduction to Quantum Computation and Information*, edited by LO H.-K., POPESCU S. and SPILLER T. (World Scientific, Singapore) 1998; FISCHER J. and LOSS D., *Science*, **324** (2009) 1277.